Heliyon 6 (2020) e05832

Contents lists available at ScienceDirect

Heliyon

journal homepage: www.cell.com/heliyon

Research article

Bioconvection due to gyrotactic microbes in a nanofluid flow through a porous medium

Sohail Ahmad [a,*], Muhammad Ashraf [a], Kashif Ali [b]

[a] Centre for Advanced Studies in Pure and Applied Mathematics, Bahauddin Zakariya University, Multan, 60800, Pakistan
[b] Department of Basic Sciences and Humanities, Muhammad Nawaz Sharif University of Engineering and Technology, Multan, 60000, Pakistan

ARTICLE INFO

Keywords:
Nanofluids
Gyrotactic microbes
Bioconvection
Thermal radiation
Porous medium

ABSTRACT

The addition of gyrotactic microbes in the nanoparticles is essential to embellish the thermal efficiency of many systems such as microbial fuel cells, bacteria powered micro-mixers, micro-volumes like microfluidics devices, enzyme biosensor and chip-shaped microdevices like bio-microsystems. Porous media also plays a pivotal role in augmentation of the thermal efficiency. Our approach in the present work is to offer a novel study of bio-convection due to gyrotactic microbes in a nanofluid flow comprising thermal radiation within a porous media over a nonlinear shrinking/stretching surface. The entire coupled system involving nonlinear equations is tackled by means of Successive over Relaxation technique. The impacts of the involved parameters on the flow, motile microbes diffusion rate, mass and heat transfer rates are examined and shown through diagrams and tables. Comparisons with graphical and tabular data are provided and observed to be in a good agreement. Numerical results evidently point out that the motile microbes parameter and the bioconvection Peclet number elevate the motile microorganisms' density whereas the thermal radiation phenomenon enhances the temperature.

1. Introduction

The nanofluid flow over shrinking/stretching sheets are much important in many industrial and technological processes such as polymer Refining, manufacturing of glass fibers, extrusion process of aerodynamics, MHD power generators, hot roll glass blasting, geothermal power extraction, metallic plates cooling process, liquefying-spinning productions, plastic and rubber sheets manufacturing, cooling process of nuclear reactors and cooling or drying process of papers [1, 2]. Nanofluids also provide much assistance in biomedical sciences. Examples incorporate nano-cryosurgery, magnetic resonance, cancer therapeutics, localized therapy, magnetic resonance imaging (MRI), labeling of cancerous tissues, nano-drug delivery and bacteriostatic activity [3]. Due to better heat transfer mechanism, nanofluids can also be utilized for detergency.

In recent times, the flow of gyrotactic microbes in nanofluids has acquired much attention among scientists and research community due to its employments in several areas of bio-technology and science. The benefits of including nanoparticles in mobile microbes suspension can be found in microvolumes, microscale mixing and nanofluid stability [4]. There is potential of utilizing microorganisms with nanofluids in various bio-microsystems, for example, the optimization of celluloses production and to evaluate toxicity of nanoparticles in chip-shaped microdevices [5, 6]. Phycocolloides like carrageenan and alginic acid are important elements of red and brown walls of algal cell and are recycled in the production of natural gas and crude oil [7]. The microorganisms also play a momentous role to improve nanofluids stability [8]. The microorganisms and nutrients are injected in oil bearing layer to sustain the variation in permeability which is also an example of bioconvection phenomena [9].

Microorganisms are used to prepare the industrial and commercial items like biofuel, biofertilizers and bioactive secondary metabolite (alcohol) etc. Algae (one of the microorganisms) are fast growing biomass and can be converted to biodiesel fuel or biofuel [10]. An important group of microbes is plant growth promoting microorganisms (PGPMs) which can survive in rhizosphere (roots) and have an ability to improve their development and inhabit the root of the plants. The PGPMs are often used in microbial fertilizers which are used to enhance the crop yield in an eco-friendly way [11]. The cyanobacteria and eukaryotic microalgae possess several unique metabolic attributes that are beneficial in biofuel production and accumulation of bioactive metabolite or alcohols [12].

* Corresponding author.
E-mail address: sohailkhan1058@gmail.com (S. Ahmad).

https://doi.org/10.1016/j.heliyon.2020.e05832
Received 6 April 2020; Received in revised form 27 May 2020; Accepted 21 December 2020

Bioconvection nanofluid flows containing gyrotactic microbes through porous media have been comprehensively studied. A bioconvective flow of motile microbes and nanoparticles inside a horizontal plate implanted in a porous media was prophesied by Aziz et al. [13]. They reported that the bioconvection parameters substantially affect the propagation rate of motile microorganisms in the flow. Zuhra et al. [14] constructed a mathematical model to investigate the flow and heat transportation of two nanoliquids (Williamson and Casson) under the influence of autocatalysis chemical reaction and gyrotactic microbes through a porous media along a vertical solid surface. The similarity transformation was utilized to solve the flow model equations and then the acquired coupled differential equations were simplified by employing the Homotopy Analysis Method (HAM). This research explained how the parameters of heterogeneous chemical reaction and porous medium decreased the flow of microorganisms. The oscillatory and non-oscillatory instability situations of nanofluid containing oxytactic microbes in a flow was probed by Kuznetsov [15], who mentioned that the stability of nanofluid can be organized by the density tempted by the fluid temperature, density stratification due to oxytactic microbes and the nanoparticles distribution. A spectral relaxation technique was used by Shaw et al. [16] to solve the coupled differential equations representing the flow of nanofluid with gyrotactic microbes. This bioconvection flow (under the simultaneous effects of MHD and viscous dissipation) was taken in a porous sphere immersed in a porous medium.

An inclusive assessment of nanoparticles flow within porous media together with gyrotactic organisms over an extending surface was conferred by Ahmad et al. [17]. A persuasive simulation technique (Successive over Relaxation) was employed to determine the numerical solutions. In this study, the novel results were talked about by means of physical interpretations. It was found that the flow as well as the skin friction increases with the effect of porosity parameter. Aurangzaib et al. [18] presented a numerical study of nanofluid flow taking the impact of gyrotactic microorganisms. Flow was taken over a convectively-heated wedge in a Darcy-Brinkman porous media. A bioconvective flow of nanofluids, in a porous medium, holding gyrotactic microbes over a stretching surface was erected by Sarkar et al. [19]. They considered the inertia effect categorized by the non-linear Forchheimer term in mathematical model. Their results spotted that the permeability parameter reduces the heat transportation rate while suction parameter amplifies the mass transportation rate. The theory regarding occurrence of bioconvection through a porous media was first spearheaded by Kessler [20], who proposed that a porous media can be utilized to concentrate the dynamic cells of chlamydomonas rosae and chlamydomonas nivalis. Moreover, Kessler [20] experimentally verified that bioconvection through a porous media (which was surgical cotton) can be used to remove fungus from Dunaliella species (unicellular species belong to phylum group like motile microalgae). These illustrations portray the significance of understanding bioconvection through porous media and investigating the impact of porous medium on bioconvection.

The purpose of recent work is to present a novel study regarding nanofluid flow containing nanoparticles and gyrotactic microorganisms towards a sheet. The available literature doesn't involve sufficient work on bioconvection of gyrotactic microbes in a nanofluid flow together with thermal radiation through a porous medium past a nonlinear shrinking/stretching surface. The outcomes, achieved by changing the relevant parameters, are illustrated and discussed by means of tables and graphs.

2. Description of mathematical formulation

We consider steady two-dimensional flow of nanofluids enclosing both nanoparticles and gyrotactic microbes through a porous medium by taking the impact of thermal radiation. The fluid concentration, temperature and concentration of the microorganisms at sheet surface are

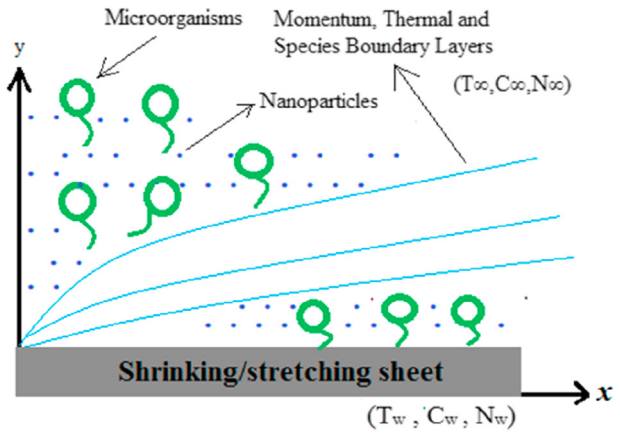

Figure 1. Geometry of the problem.

denoted by C_w , T_w and N_w (see Figure 1). No change occurs in the presence of nanoparticles for swimming path way of microbes and their velocity. But microbes motion is affected if nanoparticles volume fraction is greater than 1%. Hence, the required bioconvection stability is attained by mixing microbes and solid nano particles in the base liquid. Thermal, species and momentum boundary layers through flow regime are displayed in Figure 1.

The flow model governing equations, in case of thermal radiation and porous media, can be written as [21, 22, 23]:

$$\frac{\partial v}{\partial y}+\frac{\partial u}{\partial x}=0 \tag{1}$$

$$u\frac{\partial u}{\partial x}+v\frac{\partial u}{\partial y}=\upsilon\frac{\partial^2 u}{\partial y^2}+u_e\frac{\partial u_e}{\partial x}+\frac{\mu}{\rho k^*}(u_e-u) \tag{2}$$

$$u\frac{\partial T}{\partial x}+v\frac{\partial T}{\partial y}=\frac{\tau D_T}{T_\infty}\left(\frac{\partial T}{\partial y}\right)^2+\tilde{\alpha}\frac{\partial^2 T}{\partial y^2}+\frac{16\sigma T^3}{3k_0\rho c_p}\frac{\partial^2 T}{\partial y^2}+\tau D_B\frac{\partial C}{\partial y}\frac{\partial T}{\partial y} \tag{3}$$

$$v\frac{\partial C}{\partial y}+u\frac{\partial C}{\partial x}=D_B\frac{\partial^2 C}{\partial y^2}+\frac{D_T}{T_\infty}\frac{\partial^2 T}{\partial y^2} \tag{4}$$

$$v\frac{\partial N}{\partial y}+u\frac{\partial N}{\partial x}+\frac{1}{C_w-C_\infty}\frac{\partial}{\partial y}\left[N\left(\frac{\partial C}{\partial y}\right)\right]bW_c=D_n\frac{\partial^2 N}{\partial y^2} \tag{5}$$

The components of velocity along x and y axis are$u$and v respectively while y-axis is taken normal to the sheet. Furthermore $\rho, k^*, D_n, \tilde{\alpha}, D_B, \upsilon, \tau, T_\infty, N, T, k_0, C, \sigma, bW_c, c_p, C_\infty,$ & D_T represent the density, Darcy permeability, diffusivity of microorganisms, thermal conductivity, brownian diffusion coefficient, kinematic viscosity, nanofluid heat capacity ratio, ambient temperature, microorganism concentration, temperature, mean absorption coefficient, concentration of fluid, Stefan–Boltzmann constant, cell swimming speed, specific heat constant, ambient concentration and thermophoretic coefficient respectively. The boundary conditions at $y=0$ and at $y\to\infty$ can be given as:

$$y=0:\ u=cx^m,\ N=N_w,\ C=C_w,\ v=v_w(x),\ T=T_w \tag{6}$$

$$y\to\infty:\ u=ax^m,\ N=N_\infty,\ T=T_\infty,\ C=C_\infty \tag{7}$$

here, mass flux is denoted by v_w which relates to injection$(v_w<0)$ and suction$(v_w>0)$. Whereas $u_w(x)=cx^m$ represents stretching velocity and that of $u_e(x)=ax^m$ represents ambient velocity, where m is constant (greater than one) which implies the nonlinearity of stretching/shrinking surface. The concentration of fluid, temperature and concentration of the

microorganisms far away from sheet surface are denoted by C_∞, T_∞ and N_∞ respectively. Following dimensionless coordinates are used (see [24]) to alter the relevant PDEs (1)–(5) into ODEs:

$$\psi = \sqrt{a x^{m+1} \upsilon} f(\eta),\ \xi = \sqrt{\frac{a}{\upsilon} x^{m-1}}\, y,\ G(\eta) = \frac{N - N_\infty}{N_w - N_\infty},\ \varphi(\eta) = \frac{C - C_\infty}{C_w - C_\infty},\ \theta(\eta) = \frac{T - T_\infty}{T_w - T_\infty} \tag{8}$$

Invoking above coordinates in Eqs. (2), (3), (4), and (5), we achieve the following dimensionless equations:

$$f''' + P_0(1 - f') = m\left(f'^2 - 1\right) - \frac{1+m}{2} f f'' \tag{9}$$

$$\left[\frac{1}{\mathrm{Pr}} + \frac{4}{3}Nr\right]\theta'' + N_b \varphi' \theta' + \frac{1+m}{2} f\theta' + N_t \theta'^2 = 0 \tag{10}$$

$$\varphi'' = -\frac{N_t}{N_b}\theta'' - \frac{1+m}{2} Le f \varphi' \tag{11}$$

$$G'' + \frac{1}{2} Sc\, f\, G'(1+m) = Pe[\varphi''(\Omega + G) + G'\varphi'] \tag{12}$$

Mathematical calculations for converting PDEs (1)–(5) into ODEs (9)–(12) are provided in the appendix (supplementary content).

The boundary conditions (6) and (7) take the form:

$$\begin{aligned} &\xi = 0: \quad \theta = 1,\ \varphi = 1,\ f' = \alpha, \quad f = S = 1, \\ &\xi \to \infty: \quad \varphi \to 0, \quad G \to 0,\ f' \to 1,\ \theta \to 0. \end{aligned} \tag{13}$$

where S is suction/injection, α is an expanding (if $\alpha > 0$) or shrinking (if $\alpha < 0$) of sheet parameter and the remaining parameters included in Eqs. (9), (10), (11), and (12) are:

$$\left.\begin{aligned} &Le = \frac{\nu}{D_B}, \quad N_t = \frac{\tau D_T (T_w - T_\infty)}{\nu T_\infty}, \quad Sc = \frac{\nu}{D_n}, \quad Pr = \frac{\nu}{\alpha}, \quad \Omega = \frac{N_\infty}{N_w - N_\infty}, \\ &Nr = \frac{4\sigma T^3}{k_0 \mu c_p}, \quad P_0 = \frac{\nu x}{k^* u_e}, \quad N_b = \frac{\tau D_B (C_w - C_\infty)}{\nu}, \quad Pe = \frac{b W_c}{D_n}. \end{aligned}\right\} \tag{}$$

where Le exemplifies the Lewis number, N_t denotes the thermophoresis parameter, Sc is recognized as the bioconvection Schmidt number, Pr stands for the Prandtl number, Ω conveys the motile microbes parameter, Nr describes the thermal radiation parameter, N_b indicates the Brownian motion, P_0 refers to the porosity parameter and Pe signifies the Peclet number. The physical quantities of primary importance such as Nusselt number, local density number of motile microbes, skin friction and local Sherwood number in dimensionless form can be stated as:

$$Nu_x \mathrm{Re}_x^{-\frac{1}{2}} = -\theta'(0),\ \mathrm{Re}_x^{-\frac{1}{2}} Nn_x = -G'(0), \quad \mathrm{Re}_x^{\frac{1}{2}} C_{fx} = f''(0), \quad \mathrm{Re}_x^{-\frac{1}{2}} Sh_x = -\varphi'(0). \tag{14}$$

whereas $\mathrm{Re}_x = U_e x/\nu$ epitomizes the local Reynolds number.

3. Numerical approach

The finite difference (FD) discretization is employed to solve the nonlinear Eqs. (9), (10), (11), and (12). Some inadequacies may occur in order to determine the numerical solution of the complex dynamical models whose outer boundary conditions are located at infinity. There is no rule to guess the independent variable values that may approximate the infinity. Choosing small values of the variable may not provide the required accuracy; likewise, too large values may diverge the solution. Once in a while, the simulation techniques (to find the numerical solutions) become inconsistent for dynamical boundary value problems even for accurately guessed boundary conditions. It may be happen due to the instability of the differential equations or implicitly dependence of solutions on original initial conditions. Thereby, such type of difficulties can be tackled by exploiting the SOR method. In order to obtain a quick convergence, the SOR method is more reliable. Frankel [25] and Young [26], almost simultaneously, engrained the theory of SOR.

To solve the nonlinear fluid flow problems, some other implicit and multi-step methods can also be activated. But these techniques may consume a lot of time in computation process. Thereby, employing the SOR scheme we can tackle these kinds of inadequacies. The simulation procedure, in the recent work, is developed at $\eta = \eta_i$ (which is a particular grid point) after adjusting the finite differences with derivatives. Afterward, the succeeding system is solved iteratively by means of SOR method together with boundary conditions.

3.1. Numerical solution using SOR method

The numerical algorithm of the concerned problem is developed by using FD discretization. We reduce the order of Eq. (9) by substituting

$$f' = s = \frac{df}{d\xi} \tag{15}$$

The nonlinear Eqs. (9), (10), (11), and (12) become now:

$$s'' + P_0(1 - s) = m\left(-1 + s^2\right) - \frac{1+m}{2} f s' \tag{16}$$

$$\left[\frac{1}{\mathrm{Pr}} + \frac{4}{3}Nr\right]\theta'' + N_b \varphi' \theta' + \frac{1+m}{2} f\theta' + N_t \theta'^2 = 0 \tag{17}$$

$$\varphi'' - Le R_c \varphi = -\frac{N_t}{N_b}\theta'' - \frac{1+m}{2} Le f \varphi' \tag{18}$$

$$G'' + \frac{1}{2} Sc\, f\, G'(1+m) = Pe[\varphi''(\Omega + G) + G'\varphi'] \tag{19}$$

with BCs:

$$\begin{aligned} &f(0) = 1,\ s(0) = \alpha,\ G(0) = 1,\ \theta(0) = 1,\ \varphi(0) = 1, \\ &s(\infty) = 1,\ G(\infty) = 0,\ \theta(\infty) = 0,\ \varphi(\infty) = 0. \end{aligned} \tag{20}$$

Eqs. (16), (17), (18), and (19) take the following form after using finite differences:

$$s_i = \frac{1}{A_1}(B_1 q_{i+1} + C_1 q_{i-1} + D_1) \tag{21}$$

$$\theta_i = \frac{1}{A_2}(B_2 \theta_{i+1} + C_2 \theta_{i-1}) \tag{22}$$

$$\varphi_i = \frac{1}{A_3}(B_3 \varphi_{i+1} + C_3 \varphi_{i-1} + D_3) \tag{23}$$

$$G_i = \frac{1}{A_4}(B_4 g_{i+1} + C_4 g_{i-1} - D_4) \tag{24}$$

where

In order to acquire the numerical solution, following numerical procedure is adopted (see Ahmad et al. [27, 28]).

- An initial guess for $\widehat{s}^{(0)}, \widehat{G}^{(0)}, \widehat{\theta}^{(0)}$ and $\widehat{\varphi}^{(0)}$ is established in such a way that the boundary conditions (20) are identically satisfied.

$$A_1 = 4 + 2h^2P_0 + 2h^2ms_i,\ B_1 = 2 + \frac{1+m}{2}hf_i,\ C_1 = 2 - \frac{1+m}{2}hf_i,\ D_1 = 2h^2m + 2h^2P_0$$
$$A_2 = \left(\frac{8}{\mathrm{Pr}} + \frac{32}{3}N_r\right) - 4h^2H,\ B_2 = \frac{4}{\mathrm{Pr}} + \frac{16}{3}N_r + N_b(-\varphi_{i-1} + \varphi_{i+1}) + N_t\theta_{i+1} + (1+m)hf_i - 2N_t\theta_{i-1}$$
$$C_2 = \frac{4}{\mathrm{Pr}} + \frac{16}{3}N_r - N_b(-\varphi_{i-1} + \varphi_{i+1}) + N_t\theta_{i-1} - (1+m)hf_i,\ A_3 = 4,\quad B_3 = 2 + \frac{1+m}{2}Lehf_i, \tag{25}$$
$$C_3 = 2 - \frac{1+m}{2}Lehf_i,\ D_3 = 2\frac{N_t}{N_b}(\theta_{i+1} - 2\theta_i + \theta_{i-1}), A_4 = 2Pe(\varphi_{i+1} - 2\varphi_i + \varphi_{i-1}) + 4,$$
$$B_4 = 2 + \frac{1+m}{2}hScf_i - \frac{Pe}{2}(\varphi_{i+1} - \varphi_{i-1}),\quad C_4 = 2 - \frac{1+m}{2}hScf_i + \frac{Pe}{2}(-\varphi_{i-1} + \varphi_{i+1}),$$
$$D_4 = -2Pe\Omega(\varphi_{i+1} - 2\varphi_i + \varphi_{i-1})$$

- The Simpson's rule is employed to approximate the linear system (15). Afterward, $\widehat{s}^{(1)}$ in Eq. (21) is determined by using known $\widehat{f}^{(1)}$.
- Finite differences are used instead of the derivatives in Eqs. (16)- (19), and the subsequent system (21)–(24) is solved by the SOR scheme.
- Using the sequences $\widehat{s}^{(1)}, \widehat{G}^{(1)}, \widehat{\theta}^{(1)}$ and $\widehat{\varphi}^{(1)}$, the next series of functions are generated until the sequences $\{\widehat{s}^{(k)}\}$, $\{\widehat{G}^{(k)}\}$, $\{\widehat{\theta}^{k}\}$ and $\{\widehat{\varphi}^{(k)}\}$ converge to $\widehat{s}, \widehat{g}, \widehat{\theta}$ and $\widehat{\varphi}$ respectively.
- The iteration process is stopped when the following condition is fulfilled:

$$\max\left(\left|\left|\widehat{G}^{(k+1)} - \widehat{G}^{(k)}\right|\right|_{L_2}, \left|\left|\widehat{\varphi}^{(k+1)} - \widehat{\varphi}^{(k)}\right|\right|_{L_2}, \left|\left|\widehat{s}^{(k+1)} - \widehat{s}^{(k)}\right|\right|_{L_2}\right) < TOL_{iter}$$
$$\max\left(\left|\left|\widehat{\theta}^{(k+1)} - \widehat{\theta}^{(k)}\right|\right|_{L_2}, \left|\left|\widehat{f}^{(k+1)} - \widehat{f}^{(k)}\right|\right|_{L_2}\right)\Big) < TOL_{iter}$$

$TOL_{iter} = 10^{-11}$ is fixed throughout the calculation.

3.2. Comparison and code validation

The outcomes of numerical simulation are compared with the existing ones, as depicted in Table 1. The evaluation is assessed and noticed to be in a good agreement. This assessment assures the precision of our simulation procedure. Table 1 points out that all the physical quantities escalate with an increase in injection/suction parameter$S$.

We also compared our graphical results with the existing simulation data (see Figure 2). The comparison is found to be in a good agreement. It is noticed here that the profile of temperature escalates in the absence of gyrotactic microorganisms and porous media with an increase in Brownian motion parameter. The same increasing trend in $\theta(\eta)$ was observed by Rashidi et al. [30].

4. Results and discussions

In this section, numerical results are discussed with the help of physical interpretations. The system of Eqs. (16), (17), (18), and (19) is solved numerically with respect to BCs (20) for several estimations of the preeminent parameters. Numerical solutions are obtained via the SOR method, as suggested by Hildebrand [31]. The motile microbes density distribution $G(\xi)$, temperature$\theta(\xi)$, velocity$F'(\xi)$and concentration $\varphi(\xi)$ show asymptotic behavior for the selected values of step size ξ. It is better to examine fluid flow, mass and heat transport characteristics by assigning the values to the preeminent parameters instead of using particular domain dimensions and fluid properties; so that, the values of parameters may be adjusted in factual applications of the present work (please see Ahmad et al. [32]). Therefore, fixed values are assigned to the parameters like $\mathrm{Pr} = 6.2, P_0 = 0.6,\ Nr = 0.2,\ N_b = 0.2,\ N_t = 0.3,\ Sc = 1.5, Pe = 0.4, Le = 2,\ \Omega = 0.2,\ S = 1,\ m = 2$ and $\alpha = 0.5$ otherwise specified (in plots).

4.1. Effect of nonlinear positive constant (m) and porosity parameter (P_0)

The influence of positive constant m is to enhance the local motile microbes density as well as skin friction, as appeared in Table 2. Likewise, $Nu_x$and Sh_xalso increase with$m$.

It is presumed that the porous media doesn't ingest microbes. This is possible only if size of microbes is smaller than size of pores; in this way, neighborhood vorticity within the pores produced by the flow has no effect on microbes movement. Hence, gyrotactic mechanism of microbes is not influenced by the porous medium having high porosity (or much smaller permeability). If permeability or size of pores is not large then required concentration may not be generated by the dilute suspension for which bioconvection arises [33]. The same fact has also been discussed in a stability analysis of bioconvection presented by Kuznetsov and Avramenko [34]. They professed that only high porosity causes the bioconvection. The present results also designate that if porosity of the medium increases then better convergence can be achieved for bioconvection parameters. No evident difference is noticed in the concentration $Nn_x$of motile microbes due to the fact that the large size of pores ($0 < P_0 \leq 500$) do not ingest microorganisms (please see Table 3).

As the porosity parameter does not involve in heat as well as concentration equation, therefore, it does not affect the rates of mass and

Table 1. Numerical comparison between Nu_x and $Nn_x$for various S and $P_0 = Nr = 0$ when $\Omega = 1$, $Sc = 1$, $Pe = 1$, $N_t = 0.5$, $Le = 2$, $\mathrm{Pr} = 6.2, N_b = 0.5, m = 1$, $\alpha = -1$.

S	Nu_x			Nn_x		
	Shahid *et al.* [23]	Zaimi *et al.* [29]	Present results	Shahid *et al.* [23]	Zaimi *et al.* [29]	Present results
2.5	3.38557	3.38557	3.3859	3.38557	5.48217	5.4748
3.0	4.13260	4.13260	4.1336	4.13260	6.49841	6.4862
3.5	4.86811	4.86811	4.8698	4.86811	7.54285	7.5237
4.0	5.96672	5.59672	5.5994	5.96672	8.60180	8.5736
4.5	6.32096	6.32096	6.3248	6.32096	9.66858	9.6289

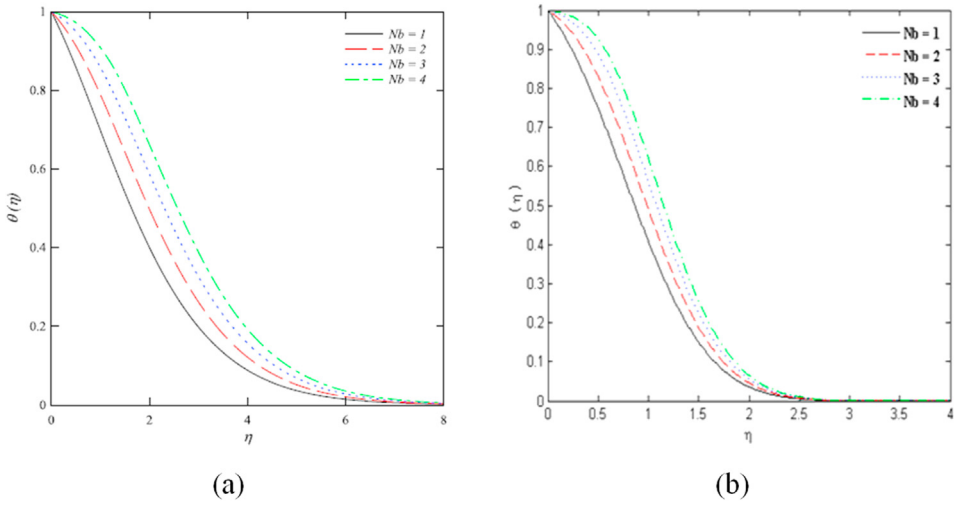

Figure 2. Temperature profiles (a) literature results [30] (b) present results for various Nb when $\Pr = N_t = 1$, $m = Le = 2$and $S = \Omega = P_0 = Nr = Pe = 0$.

Table 2. C_{fx}, Nu_x, Sh_x and $Nn_x$for various m and P_0.

m	C_{fx}	Nu_x	Sh_x	Nn_x
2	1.5231	2.6527	-0.2700	2.8226
3	1.8851	3.4493	-0.1697	3.5544
4	2.2226	4.2423	-0.0506	4.2734
5	2.5441	5.0333	0.0800	4.9863

Table 3. Impact of porosity parameter P_0 on C_{fx}, Nu_x, Sh_x andNn_x.

P_0	C_{fx}	Nu_x	Sh_x	Nn_x
0	1.4576	2.6512	0.2672	2.8167
1	1.5643	2.6541	0.2726	2.8232
10	2.2779	2.6708	0.2993	2.8577
100	5.4039	2.7116	0.3359	2.9233
200	7.3218	2.7246	0.3407	2.9396
300	8.7537	2.7316	0.3421	2.9476
400	9.9266	2.7362	0.3426	2.9526
500	10.9313	2.7396	0.3428	2.9562

heat transport significantly. Moreover, only significant change is noticed in shear stress (Table 3). It is because of the presence of P_0 in momentum equation. It is also noticed here that bioconvection through porous media is not affected in the presence of thermal radiation, and motile microbes density Nn_x is enhanced with thermal radiation effect. The outcomes reveal that Nn_x (local motile microbes density) is stable only when

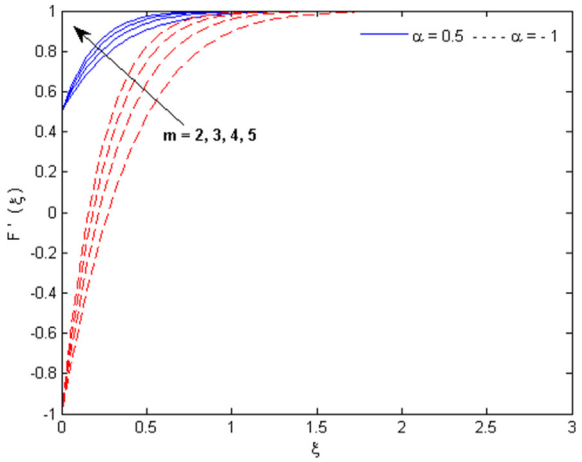

Figure 3. Velocity profile for various m and α.

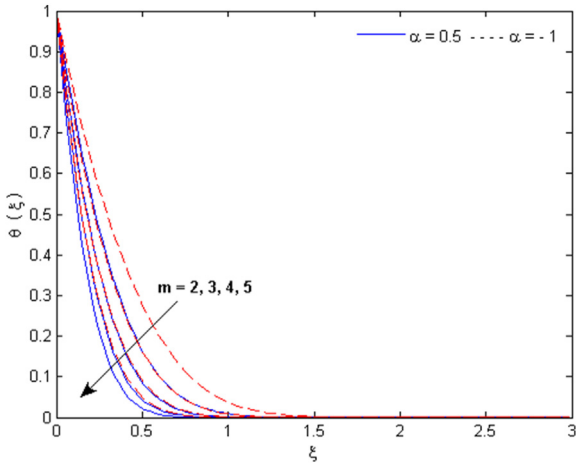

Figure 4. Temperature profile for various m and α.

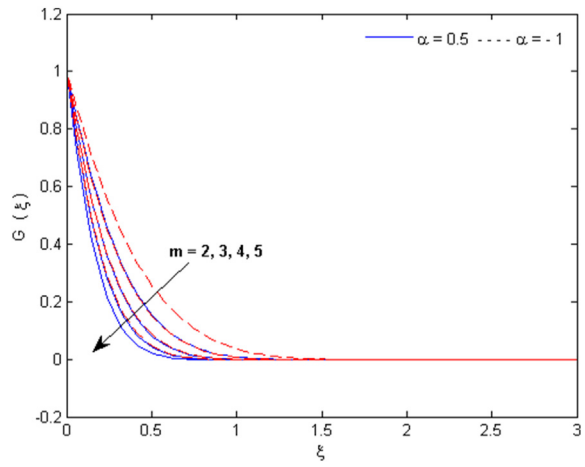

Figure 5. Motile microorganisms density profile for various m and α.

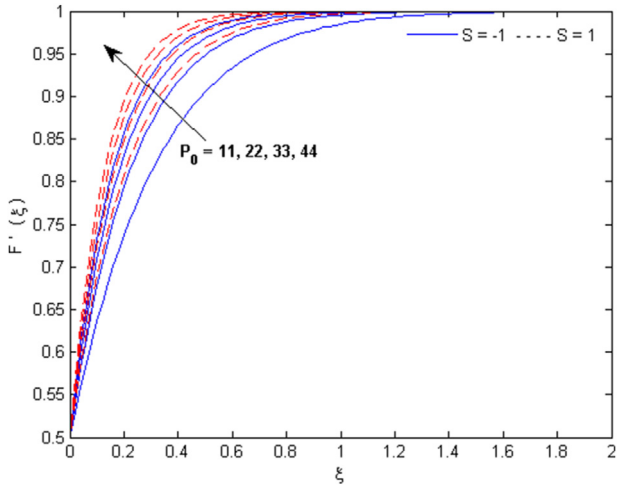

Figure 6. Velocity profile for various P_o and S.

porosity is large. In this way, our results support the results of Hill and Pedley [33]; that is, a medium or material having high porosity is appropriate for bioconvection to occur through a porous media. Our results regarding flow of gyrotactic microbes and nanoparticles through a porous media also strengthen the outcomes of Kuznetsov and Avramenko [34] about fluid flow containing oxytactic bacteria through a porous medium.

It is understandable that $\alpha = 0$ denotes the planar stagnation point flow, $\alpha = 1$ defines no boundary layer, $\alpha < 0$ describes the shrinking case and $\alpha > 0$ is correlated with the stretching of sheet.

The profiles of velocity, temperature and motile microbes density for several values of α and m are elucidated in Figures 3, 4, and 5. Both stretching ($\alpha = 0.5$) and shrinking ($\alpha = -1$) of surface together with positive constant m increase $F'(\xi)$ and decrease $\theta(\xi)$as well as $G(\xi)$across the flow regime. The flow velocity is accelerated with nonlinear stretching/shrinking cases of sheet that is appeared in Figure 3. Figure 6 exposes the effect of porosity parameterP_0 and suction/injection parameter$S$ on streamwise velocity$F'(\xi)$. An enhancement in SandP_0 tend to elevate the velocity$F'(\xi)$.

4.2. Effect of Prandtl number (Pr), thermal radiation (Nr) and thermophoretic parameter (N_t)

The values of heat transport rates for several values of Pr, $Nr$and N_t listed in Table 4 portray that the Prandtl number magnifies the rate of heat transport; however, radiation and thermophoresis parameter reduce it. The existence of the suction of fluid and nanoparticles drives the fluid towards the sheet surface and, thus, raises friction on the surface. However, as expected, heat transportation rate decreases with an increment in N_t andNr.

Temperature θ is displayed in Figures 7 and 8 for various estimations of Pr, N_t and Nr. The influence of Prandtl number is to decrease the temperature that can be seen in Figure 7. A dimensionless quantity that puts the thermal conductivity in correlation with the viscosity of a fluid refers to the Prandtl number. Pr is the ratio of thermal conductivity to the diffusivity. So, the higher Prandtl number stimulates larger diffusivity whereas the least value of Pr describes highest thermal diffusivity. This phenomenon tends to decrease the boundary layer thickness as well as the temperature. It, therefore, is not dependent on geometry of an object involved in the problem, but is dependent only on the fluid. Prandtl number is a characteristic of the fluid only [35]; so, the presence of microbes in the flow is independent of the Prandtl number.

An opposite trend (as compared to Prandtl number) is noticed in temperature profile for thermophoretic parameter and thermal radiation (see Figure 8). More heat transfers to the fluid due to increase in thermal radiation and subsequently magnifies the thermal boundary layer thickness and temperature.

The thickness of thermal boundary layer and nanofluid temperature significantly enhance with the effect of N_t. This anomaly describes that the flow is slower near the surface and faster away from the surface due to the thermophoretic force. Consequently, fluid (which is heated) moves

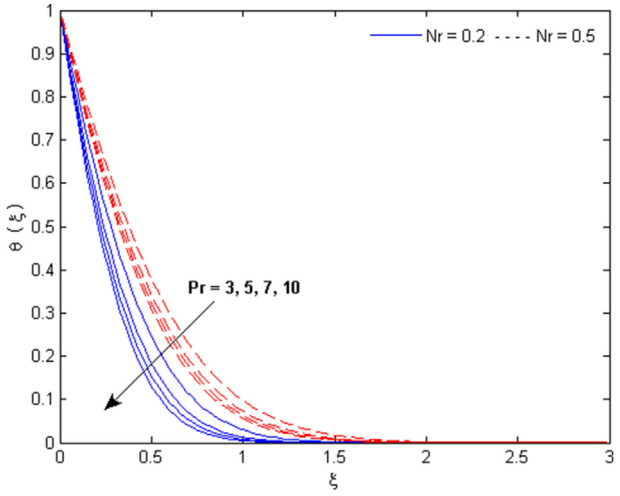

Figure 7. Temperature profile for various Pr and Nr.

Table 4. Nu_x for various Pr , Nr&N_t.

Pr	Nu_x	Nr	Nu_x	N_t	Nu_x
3	2.1498	0.2	2.6540	0.3	2.6540
5	2.5135	0.5	1.7607	0.6	2.1888
7	2.7265	0.8	1.3783	0.9	1.8156
10	2.9210	1.0	1.2203	1.2	1.5176

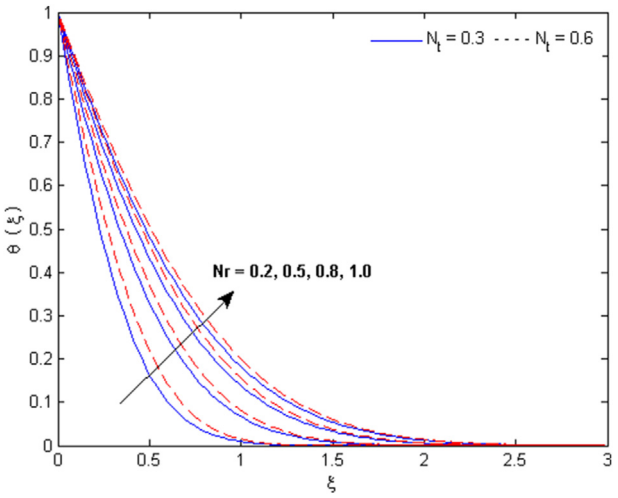

Figure 8. Temperature profile for various N_t and N_b.

away from the sheet which causes an increment in temperature. The particles shift from hotter to cooler area due to the force induced by the thermophoresis. Moreover, the high Prandtl number tends to reduce the temperature.

Most of the living organisms cannot exist at relatively very high radiation or temperature; but, some of these can survive even at a high temperature or very low temperature. For instance, better production and growth of some microorganisms such as Chlamydomonas reinhardtii and green microalgae can be acquired at extremely high temperature and these microbes are then used in the production of biodiesel. Bacteria and Archaea (which are microorganisms) can survive at high temperature. Also, water and milk involving Bacteria tolerate high temperature. Some more resistive microbes which can survive even at high radiation or temperature are lactobacilli, streptococcus aureus, streptococcus thermophiles, bifidobacteria and escheririchia coli.

4.3. Effect of bioconvection Lewis number (Le) and Brownian motion parameter (N_b)

The Lewis number*Le* and the Brownian motion parameterN_b substantially boost up the mass transport rate on surface of sheet, as appeared in Table 5. The heat transportation rate drops with the thermophoretic parameter and mass transportation rate upsurges with the Brownian motion parameter.

Figure 9 is plotted as a function of the coordinate ξ against the concentration $\varphi(\xi)$ for several$N_b$and *Le*. The outcomes of Figure 9 portray that an increment in the parameter of Brownian motion and the Lewis number tends to diminish the concentration $\varphi(\xi)$.

The profiles $G(\xi)$ as well as $\varphi(\xi)$ are marginally reduced by extending the values of *Le*. It may be due to the fact that the increasing values of the Lewis number *Le* cause a declination in mass diffusivity of nanofluid which reduces the nanoparticles concentration. Additionally, viscous diffusion rate grows as the bioconvection *Le* enhances due to which fluid speed decreases at surface of the sheet, and it causes reduction in the motile microorganisms' density distribution.

4.4. Effect of bioconvection Schmidt number (S_c), Peclet number (Pe) and motile microbes parameter (Ω)

The density of motile microbes on sheet surface increases due to bioconvection phenomenon. The effect of *Pe*, S_c and Ω is to enhance Nn_x (motile microbes' density number) on surface, as depicted in Table 6. The mass transfer occurs from sheet to the fluid if concentration of fluid is relatively low on surface than nanoparticles concentration. Therefore, an increase in Nn_x is due to the low concentration on the sheet surface. It is observed that the bioconvection parameters (S_c, *Pe* andΩ) significantly enhance the density of the motile microbes and the porous medium improves the shear stresses. The present outcomes evidently designate that the required skin friction, heat and mass transfer rates can be attained by properly choosing suction/injection velocity and the values of other parameters at the sheet surface.

The motion of the nanoparticles is because of the thermophoretic and Brownian movement. On the other hand, motion of motile microbes is self-propelled which is driven by bioconvection. Hence, motion of microorganisms is independent of the nanoparticles. A single-celled green algae (chlamydomonas) and single-celled plants (phytoplankton) can be studied as modeled gyrotactic microorganisms. Both are green coloured, photosynthetic and microscopic organisms that are beneficial to analyse the gyrotactic microbes' motion in fluid flows. These organisms are usually found in water or aquatic environment. The gravitational force causes the upward motion of chlamydomonas and phytoplankton. Self-propelled motion of these microorganisms in an aquatic environment is shown in Figure 10 (see Ahmad et al. [36]).

The unstable density stratification generates the bioconvection. In the recent work, the movement of the microbes is associated with viscous drag and gravitational torques in the flow (gyrotaxis). Figure 11 is portrayed against the motile microbes' distribution for several estimations of the bioconvection Lewis and Schmidt number. The elevating values of *Le* and *Sc*tend to depress the concentration profiles. A declaration in the

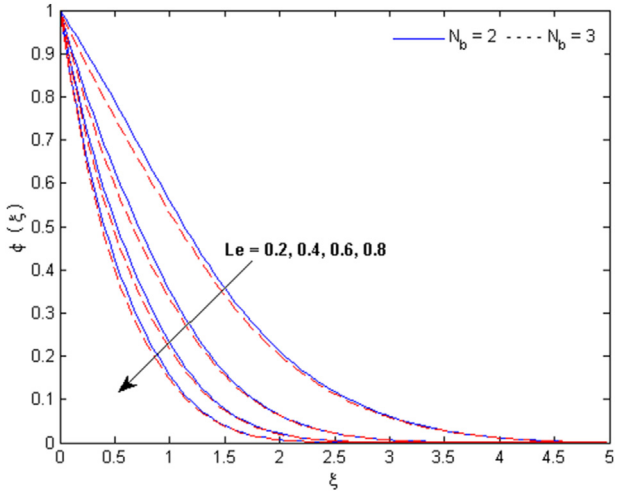

Figure 9. Concentration profile for various *Le* and N_b.

Table 5. Sh_x for various N_b and *Le*.

N_b	Sh_x	*Le*	Sh_x
0.2	0.2707	0.2	-4.2432
0.3	1.6579	0.4	-3.4624
0.5	2.7209	0.6	-2.8366
0.8	3.2515	0.8	-2.2929

Table 6. Nn_x for various S_c, $Pe$and Ω.

S_c	Nn_x	Pe	Nn_x	Ω	Nn_x
0.1	0.4764	1	2.9221	0.0	2.8293
0.2	0.6691	2	3.1289	0.2	2.8208
0.3	0.8563	3	3.3692	0.5	2.8079
0.4	1.0367	4	3.6322	0.8	2.7950

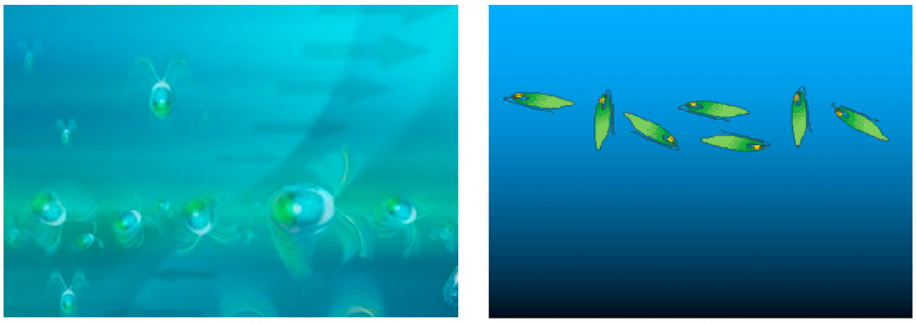

Figure 10. Motion of gyrotactic microorganisms (A) Chlamydomonas (B) Phytoplankton.

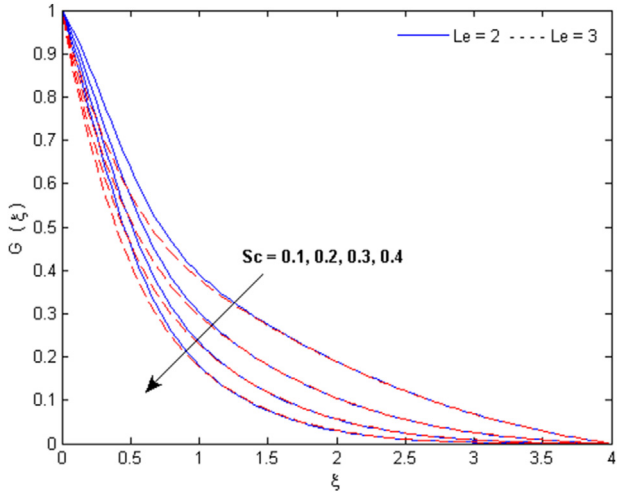

Figure 11. Motile microorganisms density profile for various *Sc* and *Le*.

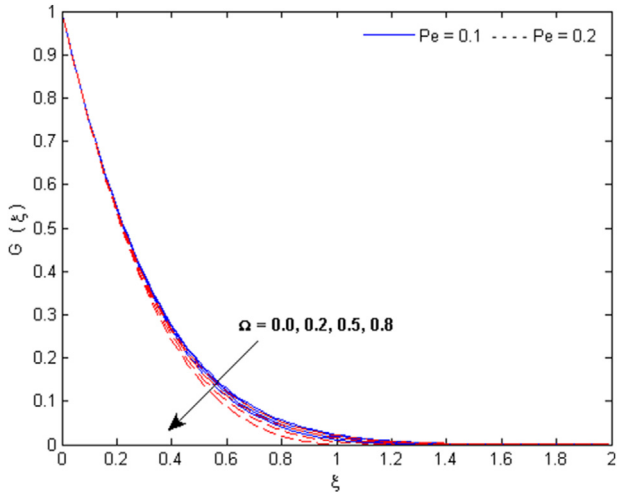

Figure 12. Motile microorganisms density profile for various Ω and *Pe*.

motile microbes distribution $G(\xi)$ is observed with an increase in the values of bioconvection Peclet number and motile microbes parameter Ω (see Figure 12).

The Peclet number Pe and cell swimming speed W_c are inversely proportional to D_n (microorganisms diffusivity) and directly proportional to each other. The rates of advection and diffusion are proportional to the Peclet number. Hence, an enhancement in the rate of advective transport gives rise to higher Peclet number which; as a result, rapidly raises the flux of the microorganisms. So, expanding values of the Peclet number depreciates the motile microbes density profile and escalates the wall motile microorganisms flux. The expanding values of the Peclet number depreciate the motile microbes density profile and increases the wall motile microbes flux. The motile microorganisms swimming rate is enhanced with the impact of bioconvection Peclet number Pe and this attribute reduces the thickness of the microorganisms near the sheet surface. It is concluded that motile microorganisms transport rate is marginally influenced in the presence of bioconvection.

5. Concluding remarks

The concerned work involves a novel study of nanofluid flow in the presence of gyrotactic microorganisms through a porous media. The thermal radiation is also taken into account in the energy equation. In order to find numerical solution, mathematical treatment is carried out via the SOR scheme. The main results may be stated as:

i. An increment in Ω, Pe and S_c (bioconvection parameters) tends to decline the density profiles and enhance the diffusion rate of microorganisms.
ii. The thermal radiation effect causes a deceleration in the heat transfer rate on sheet surface while it accelerates the temperature $\theta(\xi)$.
iii. The porous medium marginally affects the density of motile microbes and skin friction in the presence of thermal radiation.
iv. The parameters such as positive constant m (for nonlinear sheet), shrinking/stretching of sheet, suction/injection and porosity of the medium substantially elevate the dimensionless streamwise velocity.

Declarations

Author contribution statement

Sohail Ahmad: Analyzed and interpreted the data; Wrote the paper.
Muhammad Ashraf: Contributed analysis tools or data.
Kashif Ali: Conceived and designed the analysis.

Funding statement

This research did not receive any specific grant from funding agencies in the public, commercial, or not-for-profit sectors.

Competing interest statement

The authors declare no conflict of interest.

Additional information

Supplementary content related to this article has been published online at https://doi.org/10.1016/j.heliyon.2020.e05832.

References

[1] B. Sreekala, K. Janardhan, D. Ramya, I. Shravani, MHD boundary layer nanofluid flow of heat transfer over a nonlinear stretching sheet presence of thermal radiation and partial slip with suction, GJPAM 13 (9) (2017) 4927–4941.
[2] A. Shahid, H. Huang, M.M. Bhatti, L. Zhang, R. Ellahi, Numerical investigation on the swimming of gyrotactic microorganisms in nanofluids through porous medium over a stretched surface, Mathematics 8 (2020) 380.
[3] M. Bhatti Muhammad, Marin Marin, Zeeshan Ahmed, R. Ellahi, I. Abdelsalam Sara, Swimming of motile gyrotactic microorganisms and nanoparticles in blood flow through anisotropically tapered arteries, Front. Phys. 8 (2020) 95.
[4] W.N. Mutuku, O.D. Makinde, Hydromagnetic bioconvection of nanofluid over a permeable vertical plate due to gyrotactic microorganisms, Comput. Fluids 95 (2014) 88–97.
[5] Md. Tausif, S.k, D. Kalidas, P.K. Kundu, Multiple slip effects on bioconvection of nanofluid flow containing gyrotactic microorganisms and nanoparticles, J. Mol. Liq. 220 (2016) 518–526.
[6] N. Acharya, D. Kalidas, P.K. Kundu, Framing the effects of solar radiation on magneto- hydrodynamics bioconvection nanofluid flow in presence of gyrotactic microorganisms, J. Mol. Liq. 222 (2016) 28–37.
[7] A.A. El Gamal, Biological importance of marine algae, Saudi Phar. J. 18 (1) (2010) 1–25.
[8] W.A. Khan, O.D. Makinde, Z.H. Khan, MHD boundary layer flow of a nanofluid containing gyrotactic microorganisms past a vertical plate with Navier slip, Int. J. Heat Mass Transf. 74 (2014) 285–291.
[9] T.L. Stewart, H.S. Fogler, Biomass plug development and propagation in porous media, Biotechnol. Bioeng. 72 (2001) 353–363.
[10] S.P. Singh, P. Singh, Effect of temperature and light on the growth of algae species: a revie enew, Sust. Energ. Rev. 50 (2015) 431–444.
[11] S. Stamenkovic, V. Beskoski, Karabegovic Ivana, M. Lazic, N. Nikolic, Microbial fertilizers: a comprehensive review of current findings and future perspectives, Span, J. Agric. Res. 16 (1) (2018), e09R01.
[12] R. Radakovits, R.E. Jinkerson, Al Darzins, M.C. Posewitz, Genetic engineering of algae for enhanced biofuel production, Eukaryot. Cell 9 (4) (2010) 486–501.
[13] A. Aziz, W.A. Khan, I. Pop, Free convection boundary layer flow past a horizontal flat plate embedded in porous medium filled by nano-fluid containing gyrotactic microorganisms, Int. J. Therm. Sci. 56 (2012) 48.
[14] S. Zuhra, S. Noor Khan, A. Muhammad, I. Saeed, K. Aurangzeb, Buoyancy effects on nanoliquids film flow through a porous medium with gyrotactic microorganisms and cubic autocatalysis chemical reaction, Adv. Mech. Eng. 12 (1) (2020) 1–17.
[15] A.V. Kuznetsov, Nanofluid bioconvection in porous media: oxytactic microorganisms, J. Porous Med. 15 (3) (2012) 233–248.
[16] S. Shaw, S. Sandile Motsa, P. Sibanda, Magnetic field and viscous dissipation effect on bioconvection in a permeable sphere embedded in a porous medium with a nanofluid containing gyrotactic micro-organisms, Heat Transfer—Asian Res. 47 (2018) 718–734.
[17] S. Ahmad, M. Ashraf, K. Ali, Nanofluid flow comprising gyrotactic microbes through a porous medium-a numerical study, Therm. Sci. (2020).
[18] Aurangzaib, M.M. Rashidi, A.J. Chamkha, Flow of nanofluid containing gyrotactic microorganisms over static wedge in Darcy-brinkman porous medium with convective boundary condition, J. Porous Med. 21 (10) (2018) 911–928.
[19] A. Sarkar, D. Kalidas, P.K. Kundu, On the onset of bioconvection in nanofluid containing gyrotactic microorganisms and nanoparticles saturating a non-Darcian porous medium, J. Mol. Liq. 223 (2016) 725–733.
[20] J.O. Kessler, The external dynamics of swimming micro-organisms, Prog. Phycol. Res. 4 (1986) 257–307. Biopress, Bristol.
[21] A.V. Kuznetsov, The onset of bioconvection in a suspension of gyrotactic microorganisms in a fluid layer of finite depth heated from below, Int. Commun. Heat Mass Tran. 32 (2005) 574–582.
[22] F. Mabood, S. Shateyi, M.M. Rashidi, E. Momoniat, N. Freidoonimehr, MHD stagnation point flow heat and mass transfer of nanofluids in porous medium with radiation, viscous dissipation and chemical reaction, Adv. Powder Tech. 27 (2016) 742–749.
[23] A. Shahid, Z. Zhou1, M.M. Bhatti, D. Tripathi, Magnetohydrodynamics nanofluid flow containing gyrotactic microorganisms propagating over a stretching Surface by Successive Taylor Series Linearization Method, Microgravity Sci. Technol. 30 (4) (2018) 445–455.
[24] N.Z. Aini Mat, N.M. Arifin, R.M. Nazar, F. Ismail, Similarity solutions for the flow and heat transfer over a nonlinear stretching/shrinking sheet in a nanofluid, AIP Conf. Proc. 1450 (2012) 165–172.
[25] S.P. Frankel, Convergence rates of iterative treatments of partial differential equations, Math. Tables Aids Comput. 4 (1950) 65–75.
[26] D.M. Young, Iterative Methods for Solving Partial Differential Equations of Elliptic Type, Doctoral Thesis, Harvard University Cambridge, 1950.
[27] S. Ahmad, M. Ashraf, K. Ali, Numerical simulation of viscous dissipation in a micropolar fluid flow through a porous medium, J. Appl. Mech. Tech. Phys. 60 (2019) 996–1004.
[28] S. Ahmad, M. Ashraf, K. Ali, Nanofluid flow comprising gyrotactic microorganisms through a porous medium, J. Appl. Fluid Mech. 13 (5) (2020) 1539–1549.
[29] K. Zaimi, A. Ishak, I. Pop, Stagnation-point flow toward a stretchng/shrinking sheet in a nanofiuid containing both nanoparticies and gyrotactic microorganisms, J. Heat transf. 136 (2014) 1–9, 041705.
[30] M.M. Rashidi, N. Freidoonimehr, A. Hosseini, O. Anwar Beg, T.K. Hung, Homotopy simulation of nanofluid dynamics from a non-linearly stretching isothermal permeable sheet with transpiration, Meccanica 49 (2014) 469–482.
[31] F.B. Hildebrand, Introduction to Numerical Analysis, Tata McGraw-Hill Publishing Company, New Delhi, 1978.
[32] S. Ahmad, M. Ashraf, K. Ali, Simulation of thermal radiation in a micropolar fluid flow through a porous medium between channel walls, J. Therm. Anal. Calorim. (2020).
[33] N.A. Hill, T.J. Pedley, Bioconvection, Fluid Dynam. Res. 37 (2005) 1–20.
[34] A.V. Kuznetsov, A.A. Avramenko, Analysis of stability of bioconvection of motile oxytactic bacteria in a horizontal fluid saturated porous layer, Int. Commun. Heat Mass Tran. 30 (2003) 593–602.
[35] G.F. Hewitt, G.L. Shires, T.R. Bott, Process Heat Transfer, CRC Press, Boca Raton, FL, 1994.
[36] S. Ahmad, M. Ashraf, K. Ali, Heat and mass transfer flow of gyrotactic microorganisms and nanoparticles through a porous medium, Int. J. Heat Tech. 38 (2) (2020) 395–402.